Thermal metrology of water sensitive materials: experimental and theoretical approaches

Mohammad AGHAHADI[1,2], **Essolé PADAYODI**[1]*, **Saïd ABBOUDI**[2], **S. Amir BAHRANI**[3]

[1]Pôle ERCOS, ELLIADD (EA. 4661) – University of Bourgogne Franche Comté, University of Technology of Belfort-Montbéliard, 90010 Belfort (FR)
[2]ICB-COMM, UMR 6303, CNRS – University of Bourgogne Franche Comté, University of Technology of Belfort-Montbéliard, 90010 Belfort (FR).
[3]Institut Mines-Télécom Lille-Douai, University of Lille (FR)
[*](Corresponding author: essole.padayodi@utbm.fr)

Abstract - This study deals with the thermal metrology of hydrophilic and hydrophobic materials so to support the rise of bio-sourced insulators. An experimental approach based on the asymmetric hot plate method and a theoretical approach of coupled heat and humidity transfers are performed. The experimental results show that, at 20°C, the thermal conductivity λ of flax fibers insulators increases up to 20% when the relative humidity RH increases from 30% to 90%, i.e. from 0.028 to 0.033 $W.m^{-1}.K^{-1}$ while λ remains constant for the hydrophobic material. This agrees with the theoretical model results.

Keywords: thermal conductivity, coupled transfer, hot plate method, hydrophilic insulators

Nomenclature

C_p	Thermal capacity, $J.kg^{-1}.K^{-1}$
D_X^l	Isothermal mass diffusivity on liquid phase, m^2s^{-1}
D_T^l	Non-isothermal mass diffusivity on liquid phase, $m^2s^{-1}K^{-1}$
D_X^v	Isothermal mass diffusivity of on vapor phase, m^2s^{-1}
D_T^v	Non-isothermal mass diffusivity on vapor phase, $m^2s^{-1}K^{-1}$
e	Thickness, m
I	Current, A
L_v	Evaporation latent heat, $KJ.kg^{-1}$
$\dot{m}$	Rate of evaporated water per unit of time and unit of volume of medium, $kg.m^{-3}.s^{-1}$
m	Mass, kg
R	Electrical resistance, Ω
S	Surface, m^2
T	Temperature, $°C$
t	Time, s
U	Voltage, V
V	Volume, m^{-3}
X	Water vapor mass fraction
λ	Thermal conductivity, $W.m^{-1}.K^{-1}$
ρ_0	Material density, $kg.m^{-3}$
ϕ	Heat flux, W
Φ	Internal heat source, $W.m^{-3}$.
T	temperature, K
α	thermal diffusivity, $m^2.s^{-1}$

Subscripts

r	*Reference*
e	*Sample*
b	*Empty (blanc)*
l	*Liquid*
v	*Water vapor*
h	*Humid*
i	*Initial*

1. Introduction

Thermal insulators made of bio-sourced materials are being increasingly developed to cut greenhouse gas emission in building insulation. However, in spite of their interest, bio-sourced insulators have a major disadvantage related to their affinity with moisture as they are high hydrophilic materials. The classical models of thermal metrology do not match with these materials.

https://doi.org/10.25855/SFT2020-075

Indeed, firstly there are different methods for measuring the thermal conductivity of a material. These include the guarded hot plate [1], flash [2], "Hot disc" [3], hot wire, hot ribbon, tri-layer [4], hot plate methods [5, 6]. Among these, the tri-layer and hot plate methods are more suitable for characterizing low thermal conductivity materials such as bio-sourced materials [5, 6] or super insulating materials [6].

Secondly, in the case of hydrophilic materials, such as bio-sourced materials, the measurement of thermal conductivity cannot be carried out with precision unless the simultaneous transfer of heat and humidity is taken into account [7].

The objective of this study is to identify the influence of the humidity on the measurement of the thermophysical properties hydrophilic materials in a humid environment. For this purpose, an experimental approach based on the centered hot plate method and a theoretical approach based on coupled heat and humidity transfers are performed.

2. Experimental approach

2.1. Water sensitive and non-sensitive media

The hydrophilic versus hydrophobic distinction is justified when coupled heat-humidity transfer is studied. The experimental approach is thus performed on a hydrophilic insulator made of flax fibers (LFB) and on a hydrophobic material made of a phase change polymer (PCM) (*Rubitherm® paraffin*) with solidification temperature approximatively 27 °C (*Fig. 1*).

The contact angles of LFB and PCM measured by the droplet analysis are respectively θ_{PCM}=112° ±2° and θ_{LFB} = 78° ±2° (*Fig. 1c* and *1d*), showing that the surface of LFB media is wettable (as $\theta_{LFB} < 90°$) while the PCM surface is non-wettable (as $\theta_{PCM} > 90°$). The latter is hydrophobic and the LFB media is hydrophilic and could uptake the ambient humidity [8, 9]. This is confirmed by the water uptake test. The water uptake measurement is performed in a climatic chamber (*Dycometal®, CCK 480*) according to the french standard *NF EN ISO 12571*. The Figure 2 plots the evolution of the water content of the LFB sample for different relative humidity HR of the ambient air.

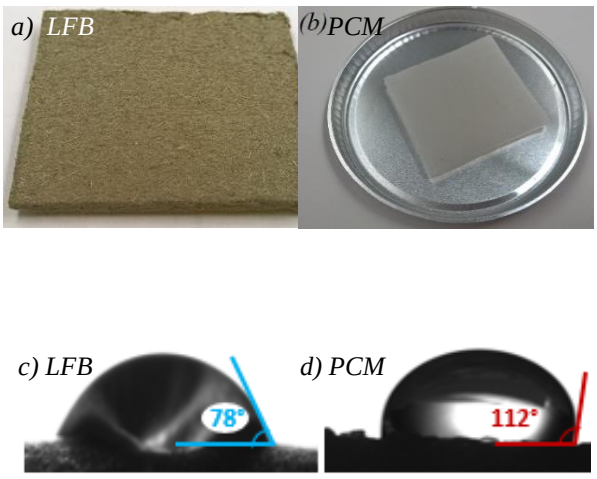

Figure 1: *Contact angle (water droplet) on the PCM and the LFB samples*

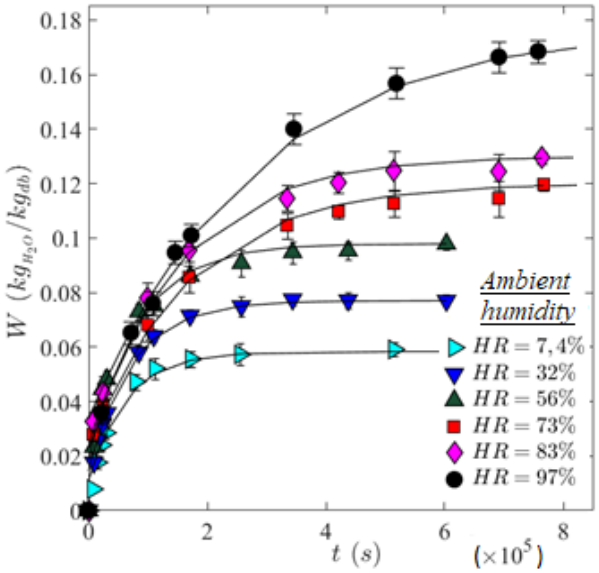

Figure 2 : *Variation of the water content of the LFB sample in atmospheres at variable relative humidity*

Clearly, the material LFB can uptake until 17 % *wt* of the humidity when lying in an ambient air at 97% HR. Bio-sourced materials are highly hydrophilic, as the result, coupling heat and humidity transfer is required when applying thermal metrology to biobased insulators.

2.2. Device for thermal conductivity measurement

An "asymmetrical centered hot plate" device (Fig. 3) [10, 11] was used to measure the thermal conductivity of the studied samples. It consists of a 21 Ω flat heating element of 46 × 46 mm² and 0.15 µm thickness (*Omega®, KHLV-202/10-p*) which is inserted between the sample to characterize and a reference sample with a well-known thermal conductivity (λ_2 = 0.069 W.m^{-1}.K^{-1}). Samples are compressed (pressure ≈ 6×10^{-2} MPa) between two identical aluminum blocks. K-type thermocouples record the evolution of interfaces temperatures $T_c(t)$, $T_0(t)$ and $T_1(t)$ (Fig. 3a). The heating element is connected to a power supply (*AIM-TTI®, PLH250-P, UK*) and thermocouples are connected to an acquisition unit (*Omega®, TC-08, UK*).

The test is carried out on low-thickness samples (≈ 4 mm) to allow a unidirectional heat flux across the sample, from one side to the other, and to minimize the lateral heat losses.

The hot plate device provided with samples is arranged in the climate Chamber (Fig. 3b) allowing to set the ambient atmosphere at a given temperature and humidity.

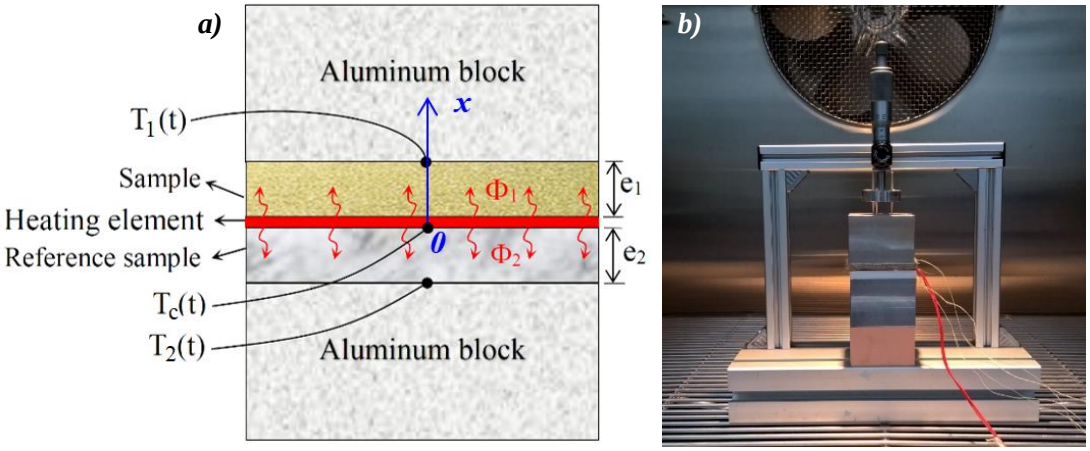

Figure 3: *Schematic layout of the "asymmetrical centered hot plate" (a) experimental device arranged in a climatic chamber (b).*

2.3. Measuring protocol

When a voltage (U = 2.33 V) and a current (I = 0.11 A) are applied, a heat flow ($\phi = U^2/R.S$) is generated through samples. The interface temperatures $T_c(t)$, $T_1(t)$ and $T_2(t)$ are then recorded until the stationary regime is reached (after approximately 3 hours). By neglecting the lateral heat loss, the generated flux (ϕ) is the sum of both heat fluxes ϕ_1 and ϕ_2, passing through each sample :

$$\phi = \phi_1 + \phi_2 \tag{1}$$

In a stationary regime, the Fourier's law of heat conduction allows us to write :

$$\begin{cases} \phi_1 = \frac{\lambda_1}{e_1}(T_c - T_1) \\ \phi_2 = \frac{\lambda_2}{e_2}(T_c - T_2) \end{cases} \tag{2}$$

The thermal conductivity λ_1 of the sample is deduced from the above equations as follow :

$$\lambda_1 = \frac{e_1}{T_c - T_1}\left[\frac{U^2}{RS} - \frac{\lambda_2}{e_2}(T_c - T_2)\right] \quad (3)$$

For the LFB sample, measurements are taken at relative humidity conditions of 30%, 50%, 70% and 90% RH, the temperature being maintained for each RH case at 20 °C, 30°C, 40 °C and 50 ° C. For the PCM sample, measurements are performed at extreme RH of 30% and 90% and at 10°C and 15 °C, i.e, below the phase change temperature of PCM (27°C).

2.4. Experimental determination of thermal capacity and absolute density

As the thermal capacity and the absolute density are involved in the coupled heat-humidity transfers, these parameters are previously measured on the LFB and PCM samples. The density is determined by the hydrostatic weighing method using a balance and the thermal capacity is measured by the continuous temperature programming method using the DSC calorimeter (*TA Instrument®, Q20, USA*), as well detailed in our previous paper [12]. The thermal capacity of the sample C_{p_e} is then calculated from the correlation:

$$c_{p_e}(T) = c_{p_r}(T)\ \frac{\phi_e - \phi_b}{\phi_r - \phi_b}\ \frac{m_r}{m_e} \quad (4)$$

Where C_{p_r}, m_r and ϕ_r are respectively the heat capacity, the mass and the heat flux of the reference sample, m_e and ϕ_e, the mass and the heat flux of the sample to be characterized and ϕ_b the thermal flux of the empty sample holder.

Experimental results of C_{p_e} are plotted on Figure 4.

3. Theoretical approach of coupled heat and humidity transfers

3.1. Analytical model of coupled heat-humidity transfers

When a heat source is applied to a hydrophilic medium lying in a humid atmosphere, heat and moisture transfer phenomena occur simultaneously through this medium. The present study proposes a coupled heat and humidity transfers model that will be compared to the permanent hot plate measurement method applied to a porous sample within a humid atmosphere.

As the heat transfer can be assumed to be unidirectional at the center of the sample, according to *Ox* direction (Fig. 3), the coupled heat-humidity transfers can be considered as a one-dimensional problem.

The moisture and heat balance equations are then:

- *Mass balance (liquid and vapor phases):*

$$\rho_0 \frac{\partial X_l}{\partial t} = \frac{\partial}{\partial x}\left[\rho_0 \left(D_X^l \frac{\partial X_l}{\partial x} + D_T^l \frac{\partial T}{\partial x}\right)\right] - \dot{m} \quad (5)$$

$$\rho_0 \frac{\partial X_v}{\partial t} = \frac{\partial}{\partial x}\left[\rho_0 \left(D_X^v \frac{\partial X_v}{\partial x} + D_T^v \frac{\partial T}{\partial x}\right)\right] + \dot{m} \quad (6)$$

where D_X^l and D_X^v are isothermal mass diffusivity of liquid phase and of vapor phase respectively $(m^2 s^{-1})$ and D_T^l and D_T^v are non-isothermal mass diffusivity of liquid phase and vapor phase respectively $(m^2 s^{-1} K^{-1})$ and *T*, the temperature, *X*, the water content and $\dot{m}$, the quantity of evaporated water per unit of sample volume and per unit of time.

By summing both equations, the total mass balance of the two phases is :

$$\frac{\partial X}{\partial t} = \frac{\partial}{\partial x}\left[\left(D_X \frac{\partial X}{\partial x} + D_T \frac{\partial T}{\partial x}\right)\right] \quad (7)$$

where $D_X = D_X^l + D_X^v$ and $D_T = D_T^l + D_T^v$ (8)

In the vapor phase, by neglecting the accumulation term over the transport term, $\dot{m}$ *becomes* :

$$\dot{m} = -\frac{\partial}{\partial x}\left[\rho_0 \left(D_X^v \frac{\partial X_v}{\partial x} + D_T^v \frac{\partial T}{\partial x}\right)\right] \quad (9)$$

As the thermal diffusion can be neglected over the mass diffusion ($D_T^v \ll D_X^v$), $\dot{m}$ *becomes* :

$$\dot{m} = -\frac{\partial}{\partial x}\left(\rho_0 D_X^v \frac{\partial X_v}{\partial x}\right) \quad (10)$$

- *Heat balance*

On a macroscopic scale, by neglecting the kinetic energy and the assumption that water adsorbed in the pores is not a separate phase and by introducing the heat capacity at constant pressure, the equation of energy is :

$$\rho C_P^* \frac{\partial T}{\partial t} = \frac{\partial}{\partial x}\left[\lambda^* \frac{\partial T}{\partial x} + \rho_0 D_X^v L_v \frac{\partial X_v}{\partial x}\right] \quad (11)$$

Where λ^* and C_P^* are respectively the apparent thermal conductivity and the apparent heat capacity of the sample and L_v, the latent heat of vaporization estimated as :

$$L_v = 2495 - 2.346\,T \quad (12)$$

- *The initial and boundary conditions, referring Figure 3, are defined as :*

$$\text{At } t = 0, \begin{cases} X = X_i \\ \mathrm{T} = T_i \end{cases} \quad (13)$$

$$\text{At } t > 0 \text{ and } x = 0, \begin{cases} \frac{\partial X_l}{\partial x} = 0 \\ -\lambda \frac{\partial T}{\partial x} = \phi \end{cases} \quad (14)$$

$$\text{At } t > 0 \text{ and } x = e_1, \begin{cases} \frac{\partial X_l}{\partial x} = 0 \\ T = T_i \end{cases} \quad (15)$$

X_i and T_i are respectively the equilibrium water content and the temperature of the sample with the climatic chamber atmosphere. The eq. 15 implies that the mass transfer flux is null at the sample and the aluminum block interface and is assumed to be isothermal over time.

3.2. FE modeling of coupled heat-humidity transfers

A finite elements (FE) simulation using COMSOL Multiphysics® software is implemented to solve equations 7 and 11 with the associated boundary conditions 13, 14 and 15. Tables 1 gives the experimental and literature values of parameters involved in the mathematical and in the FE simulations.

	Density ρ_0	Thermal capacity $C_p{}^*$	Thermal conduct. λ	Mass diffusion. D_X^v	Water content X_i
LFB sample	$(kg.m^{-3})$	$(J.kg^{-1}.K^{-1})$	$(W.m^{-1}.K^{-1})$	$(m^2 s^{-1})$	----
T_i =30°C / HR=30%	988	1660	0.030	2.78×10^{-9}	0.08
T_i =40°C / HR=90%	988	1524	0.039	4.65×10^{-10}	0.17
PCM sample					
T_i =10°C / HR=90%	867	1038	0.201	---	---
T_i =15°C / HR=90%	867	2676	0.217	---	---

Table 1: *Thermophysical properties (ρ_0, $C_p{}^*$, X_i and λ are experimentally measured while D_X^v is average values of bio-sourced materials from literature [12])*

4. Results and discussion

4.1. Thermophysical characteristics

Figure 4 plots the thermal capacity C_{p_e} values of LFB and PCM samples measured experimentally. The thermal capacity of PCM increases significantly when approaching the phase change temperature, i.e. 27 °C, plummets at 27 °C as the PCM changes phase from solid state to liquid state, and increases slowly beyond. Contrary to what may be expected, the C_{p_e} of LFB decreases slightly with the increasing temperature (from 2245 ± 20 J.kg^{-1}.K^{-1} at 5 °C to 1365 ± 20 J.kg^{-1}.K^{-1} at 50 °C). The decrease of the thermal capacity of LFB is related to the loss of humidity of the sample as the latter undergoes a dehydration when the temperature increases, another perturbation of the thermal metrology when applied to hydrophilic materials.

On the other hand, the experimental values of the thermal conductivity λ of the LFB sample plotted in Figure 5, show an increase of λ with increasing temperature (+22% when the temperature increases from 20 °C to 50 °C). Indeed, the arrangement of the hot plate in the climatic chamber at a given humidity during the measurement of λ reduces the sample dehydration when the temperature increases. The results of Figure 5 show also that at a given temperature, the increase of the relative humidity leads to the thermal conductivity increasing (at 20 °C, by increasing the relative humidity from 30% RH to 90% RH, λ increases from 0.028 W.m^{-1}.K^{-1} to 0.033 W.m^{-1}.K^{-1}, a rise of 18%). Clearly, the humidity transfer contributes to the heat transfer.

Table 2 shows the results of the thermal conductivity measured on the PCM materials using the hot plate. In atmospheres at 30 %HR and 90 %HR, the thermal conductivity does not vary at 10 °C ($\lambda \approx 0$, 20 W.m^{-1}.K^{-1}) or at 15 °C ($\lambda \approx 0$, 22 W.m^{-1}.K^{-1}), corroborating thus the inaction of moisture on hydrophobic materials, contrary to what has been observed above with LFB.

These results confirm the necessity to consider the coupled heat and humidity transfers when measuring thermophysical characteristics of hydrophilic materials.

The values of the thermal conductivity of PCM samples measured using the hot plate have been compared to the measurements performed with a commercial apparatus (*TA Instrument®, DTC 300, USA*) (Table 2). The results given by the commercial apparatus showed a low difference (< 2%) with those measured with the hot plate device. The latter is then validated.

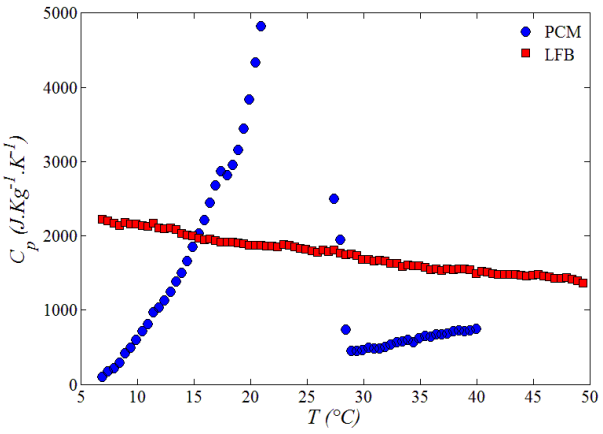

Figure 4: *Variation of the heat capacity of PCM and LFB materials according to temperature*

	Hot plate		*DTC 300*
RH	30%	90%	*50%*
at T_i=10°C	0.198	0.201	*0.201**
at T_i=15°C	0.219	0.217	*0.216**

Table 2: *Thermal conductivity of the PCM material at different temperatures T_i and relative humidity measured using the hot plate.* **Comparison to the values measured using the conductivimeter DTC 300*

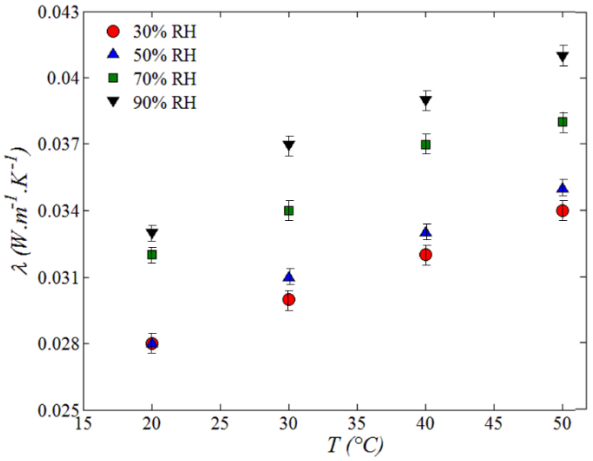

Figure 5 : *Thermal conductivity variation of the LFB material as a function of temperature for different relative humidities.*

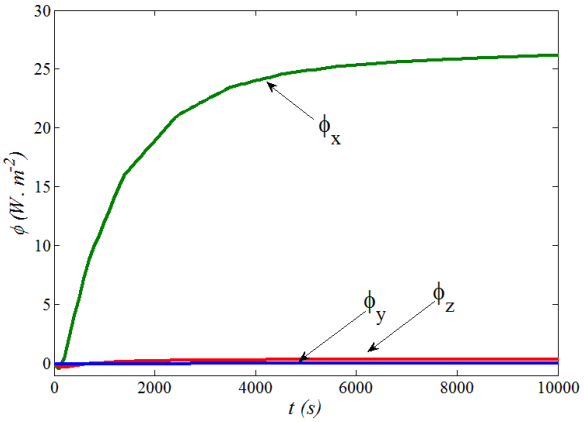

Figure 6 : *Heat flux variation computed by COMSOL Multiphysics.*

4.2. Numerical results

First, to verify the assumption of a unidirectional heat transfer in the center of the sample when arranged in the hot plate, the heat fluxes ϕ_x, ϕ_y and ϕ_z according to *Ox, Oy and Oz* directions given by the FE modeling at the center of the sample are compared on Figure 6. As one can see, the heat fluxes ϕ_y and ϕ_z are almost null while the heat flux ϕ_x increases up to 27 W.m^{-2} when the hygro-thermal equilibrium is established. This validates the unidirectional heat transfer hypothesis.

Figures 7a and 7b show a comparison between the experimental and calculated temperatures $\Delta T(t) = T_0(t) - T_i$ on the rear face of the PCM and LFB samples, respectively. In the case of the hydrophobic material, the latent heat of vaporization L_v is considered nil, thus the coupling term in the coupled system of equation 11 is canceled. The equation becomes a simple heat transfer problem.

In both cases, a good correlation was observed between the experimental and the numerically simulated curves (the difference between the experimental and the simulated curves is approximately 4%). So, one can consider that the proposed model of coupled heat-humidity transfers is validated.

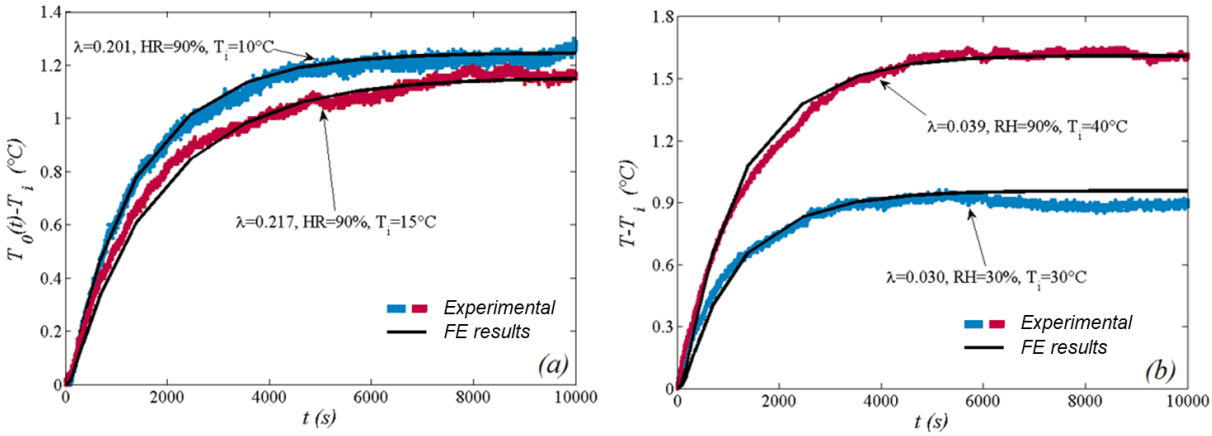

Figure 7: *Comparing of the experimental and the calculated temperatures on the rear face of the sample (a) PCM and (b) LFB.*

5. Conclusion

An experimental study and a theoretical approach are investigated to analyze the influence of humidity on the thermal metrology of hydrophilic materials. The experimental characterization using a centered hot plate showed a high influence of the humidity on the thermal conductivity of a hydrophilic insulator made of flax fibers (LFB). Around the ambient temperature, the thermal conductivity of this thermal insulator can rise about 18 % when the ambient relative humidity increases from 30 % to 90 %. 0n the other hand, the relative humidity variation does not impact the thermal conductivity of the hydrophobic material (PCM).

Clearly, the measure of the thermo-physical properties of hydrophilic materials requires models considering the influence of the humidity. A simultaneous heat and moisture transfers coupling heat and mass balance equations by the latent heat of vaporization has been proposed in this study. The equation of the coupled heat and humidity transfers model is solved in *1D* Cartesian coordinate using COMSOL Multiphysics®software. The results show a good agreement between the simulated values and the experimental measurements with a deviation of less than 4%. This model is suitable for both hydrophilic and hydrophobic materials, as for the latter, it's lack in humidity leads to a nil latent heat of vaporization and the coupled heat and humidity transfers model becomes a pure heat transfer model.

References

[1] T. Kobari, J. Okajima, A. Komiya, S. Maruyama, Development of guarded hot plate apparatus utilizing Peltier module for precise thermal conductivity measurement of insulation materials, Int. *J. Heat Mass Transf.*, 91 (2015), 1157–1166.

[2] A. Degiovanni, M. Laurent, Une nouvelle technique d'identification de la diffusivité thermique pour la méthode « flash », *Rev. Phys. Appliquée*, 21 (1986), 229–237.

[3] Y. Jannot, Z. Acem, A quadrupolar complete model of the hot disc, Meas. *Sci. Technol.*, 18 (2007) 1229–1234.

[4] S.A. Bahrani, Y. Jannot, A. Degiovanni, Extension and optimization of a three-layer method for the estimation of thermal conductivity of super-insulating materials, *J. Appl. Phys.*, 116 (2014),

[5] Y. Jannot, V. Felix, A. Degiovanni, A centered hot plate method for measurement of thermal properties of thin insulating materials, *Meas. Sci. Technol.*, 21 (2010) 035106.

[6] V. Félix, Caractérisation Thermique de Matériaux Isolants Légers Application à des Aérogels de Faible Poids Moléculaire. Ph.D. thesis, 2011.

[7] H. Bal, Y. Jannot, N. Quenette, A. Chenu, S. Gaye, Water content dependence of the porosity, density and thermal capacity of laterite-based bricks with millet waste additive, *Constr. Build. Mater.* 31 (2012) 144–150,

[8] K-E. Atcholi, E. Padayodi, J-C. Sagot, T. Beda, O. Samah, J. Vantomme, Thermomechanicalbehavior of the structures of tropical clays from Togo (West Africa) fired at 500 °C, 850 °C and 1060°C, *Constr. Build. Mater,* 27 (2012) 141–148.

[9] D. Quere, *Les surfaces super-hydrophobes,* Images la Phys., 239–244.

[10] N. Laaroussi, A. Cherki, M. Garoum, A. Khabbazi, A. Feiz, Thermal properties of a sample prepared using mixtures of clay bricks, *Energy Procedia,* 42 (2013) 337–346.

[11] Y. Jannot, A. Degiovanni, V. Grigorova-Moutiers, J. Godefroy, A passive guard for low thermal conductivity measurement of small samples by the hot plate method, *Meas. Sci. Tech. 28*(2017) 15008

[12] M. Aghahadi, E. Padayodi, S. Abboudi, S.A. Bahrani, Physical modeling of heat and moisture transfer in wet bio-sourced insulating materials, *Review of Sci. Instruments* 89, 104902 (2018).